Journal of Control, Automation and Electrical Systems (2019) 30:1041–1050
https://doi.org/10.1007/s40313-019-00507-5

Loading Margin Sensitivity in Relation to the Wind Farm Generation Power Factor for Voltage Preventive Control

Victor R. Neumann Silva[1] · **Roman Kuiava**[2]

Received: 8 April 2019 / Revised: 24 June 2019 / Accepted: 3 August 2019 / Published online: 14 August 2019

Abstract
Due to the growing importance of wind farms in the electric power generation matrix in many countries, for example, in Brazil, this paper proposes voltage preventive control actions as an activity to support the programming of the operation of the electric system, based on the ranking of wind power units that most significantly impact the system's loading margin through the control of its power factor. A sensitivity index is proposed to obtain this ranking, whose mathematical formulation is based on a linear approximation of the power balance equations in the vicinity of the maximum loading point. The system used to test this proposal is a 56-bus system prepared with current real data from the Northeast subsystem of the National Interconnected System of Brazil that includes 22 wind farms with 234 wind turbines, which comprise a total of 600 MW of installed capacity. The results obtained for the 56-bus test system show the applicability of the proposed voltage preventive control actions by indicating the wind farms that can contribute most significantly to the increase in the system's loading margin from an adequate adjustment of the power factor of these units.

Keywords Voltage preventive control · Wind farms · Sensitivity analysis · Loading margin · Modified power factor · Saddle-node bifurcation

1 Introduction

Points of interconnection (POIs) can represent reactive power reservoirs when the renewable generation coupled to the system, mainly at the sub-transmission level, comes from wind or solar photovoltaic, and may lead to diverse consequences on system stability, as highlighted in Baghsorkhi (2015). In contrast, Tamimi et al. (2011) mentions that the behavior of photovoltaic generation in the electric grid is determined by the way the active and reactive output powers are controlled by the inverters, allowing the control of the voltage magnitude in the POI. Other studies point out that if the coupled distributed generation is from plants with synchronous generators, which may be from small hydroelectric power plants or thermoelectric generators, the control variables of these generators (Greene et al. 1997), such as power factor (PF) adjustment (Hatziargyriou et al. 2017), could be used as resources that contribute to the stability of the electrical system, or at least in the vicinity of the POI.

Nowadays, due to the growing importance of wind farms in the electric power generation matrix in many countries, and especially in Brazil, it is fundamental to deepen the studies about their behavior during possible disturbances in the grid and, as one of the objectives of this paper, how the coupling of wind farms to the electrical system can contribute to mitigate voltage stability problems. Several studies have proposed the use of reactive power generation capacity of wind farms to improve the transient stability of the power system (PES) for the improvement in fault ride-through (FRT) to reduce losses of the system and to attenuate the voltage fluctuations (Abdelrahem and Kennel 2016; Meegahapola et al. 2010, 2013; Konopinski et al. 2009). In this context, the main contribution of this paper, compared with these studies, is a proposal of a voltage preventive control using the resources of reactive power generation of the wind farms. This voltage preventive control is based on the wind power units that

✉ Victor R. Neumann Silva
vneumann@ufpr.br

Roman Kuiava
kuiava@eletrica.ufpr.br

[1] Department of Engineering and Exact Sciences, Federal University of Parana, R. Pioneiro, 2153, Palotina, PR ZIP 85950-000, Brazil

[2] Department of Electrical Engineering, Federal University of Parana, P.O. Box 19011, Centro Politecnico, Curitiba, PR ZIP 81531-980, Brazil

most significantly impact the system's loading margin (LM) through the control of its power factor, being the LM defined as the distance from the current load of the system up to maximum value that represents the maximum load point (MLP).

In order to discuss the potentiality of wind farms for PES voltage stability improvements, this paper analyzes the evolution of the technologies of the wind turbines from the perspective of their capability curves that relate the active and reactive powers feasible to be generated in a narrow range of power factors. This is done especially for the doubly fed induction generator (DFIG) once it is currently the most used variable speed wind turbine in wind farms, as it can be seen in Brazil. These wind turbine capability curves are related to the maximum power point tracking (MPPT) (Konopinski et al. 2009; Lund et al. 2007), and this relationship with a wind turbine can be extended to a wind farm.

In relation to the voltage preventive control, which deals with actions that must be taken in order to increase the system's loading margin (Van Cutsem 2000), it is based on the concept of static voltage stability (Colombari et al. 2019). This concept is based on the bifurcation theory (Seydel 2009), which explains the phenomena that lead the system to the voltage instability (or voltage collapse) as the load grows (Gao et al. 1992). Then, as a countermeasure to prevent such phenomenon, this paper proposes as voltage preventive control actions based on a sensitivity index of the load margin to the wind farm power factor, to select those wind farms which better contribute in the voltage static stability.

The sensitivity index, which is an innovation proposed in this paper, adopts a modified power factor definition, which is a continuous, differentiable and monotonically decreasing function of the reactive power, and so overcomes the problem of discontinuity in the conventional definition of power factor when the reactive power is zero (Cimino and Pagilla 2016; Tarchala 2011). This power factor formulation is then used in the proposed sensitivity formulation, which is based on a linear estimate of the variation of the loading margin with respect to the PF of a wind farm of interest. The basis of the proposed sensitivity index is given by Greene et al. (1997).

Therefore, the proposed index allows to classify the units that can contribute more significantly to the voltage preventive control. This sensitivity index is tested in a pertinent real scenario which is a part of the NE subsystem of SIN which comprises 22 wind farms. So, the research was focused on the DFIG wind turbine model because it is highly used in these wind farms, which delimits the wind turbine technology used in this paper.

This paper is divided into six parts: In Sect 2, the technologies of wind turbines are presented concisely, as well as DFIG wind farm modeling; in Sect. 3 is discussed the static voltage stability assessment; in Sect. 4, the formulations of the approximate modified power factor and the proposed sensitivity index are developed; in Sect. 5 are presented and discussed the results; and in Sect. 6, the conclusions are given.

2 Wind Power Generation Fundamentals for Voltage Stability Assessment (VSA)

In this section, the technologies of wind turbines are presented concisely, indicating their MPPT modeling and techniques, as well as the wind farm capabilities and bus modeling for static VSA.

2.1 Evolution of Wind Turbine Technologies

Wind power conversion technology has evolved rapidly over the last two decades with the development of power electronics-based converter systems, from the simple-fed induction generator (SFIG) and the fixed-speed wind generator (FSWG) that do not support reactive power even if they are a reactive power consumer. Being these machines replaced by variable speed wind turbines such as the permanent magnet synchronous generator (PMSG), the doubly fed induction generator (DFIG) and the full-converter wind generator (FCWG). The capacities to control both active and reactive powers, coupled with low-voltage ride-through (LVRT) and fault ride-through (FRT), are the main reasons for the intensification of the adoption of power electronics-based turbines (Meegahapola et al. 2013).

2.2 MPPT Modeling and Techniques

Although the wind has naturally variable and intermittent characteristics, for the production of electric energy it is intended that a wind turbine operates at a maximum power for each intensity of the wind speed. Considering that the wind speed can vary between the velocity of cut-in (between 5 and 6 m/s), v_0, and the velocity of cut-out (around 20 m/s), $v_{\max}$, the two main modes of operation for turbine control: the first mode, called MPPT, between v_0 and v_N (nominal wind speed where maximum power generation is achieved), and the second mode, by controlling the wind turbine blade angle, to constant and nominal power, between v_N and $v_{\max}$ can be defined. In the wind power conversion system, the electric power generated depends on the wind speed, v, the speed of the generator, ω_G, consequently on the specific speed (TSR—tip speed ratio), λ_{TSR}, and the pitch angle, β, of the wind turbine propeller blades. The λ_{TSR} represents the relationship between wind turbine blade tip speed v_{pp} [m/s] and wind speed v [m/s], formulated as $\lambda_{\mathrm{TSR}} = \frac{v_{\mathrm{pp}}}{v} = \frac{\omega_T R}{v}$, where ω_T [rad/s] is the angular speed of the turbine blade and R [m] is the radius of blades.

It is possible to obtain the maximization of the power generated by the optimization of the parameters that determine λ_{TSR}, which naturally excludes wind speed. Thus, over the last few years, MPPT algorithms have been developed to optimize one of the aforementioned parameters. These algorithms can be classified according to their control objectives which have been developed, fundamentally, for a fixed pitch angle, β, which are TSR control, power signal feedback (PSF), optimal torque control (OTC) and hill climb search control (HCS), detailed in Raza et al. (2008) and Simoes et al. (1997).

A balance between MPPT rate and control efficiency is desired. This balance is the function of the adaptive pitch controller that includes the HCS control systems. The control system of a wind turbine based on the fuzzy logic has been initially proposed by Simoes et al. (1997), which also includes the adaptive controller that determines the climb strategy and the size of the step in the search for the point of maximum power extraction, in which other variants or evolutions of the HCS are based, such as those proposed by Sl-Subhi et al. (2017), Lalouni et al. (2014) and Raza et al. (2008).

A control technique for DFIG wind turbines proposes the MPPT as part of a multi objective predictive model with active and reactive powers as the control objectives, fast grid synchronization, smooth grid connection and flexible power regulation (Hu et al. 2019).

As there is a relationship between the MPPT and the capability curves of the DFIG wind turbine, and this relation with a wind turbine can be scaled to a wind farm, in the sequence the capability curves of the DFIG are presented, as a variable speed wind turbine is considered.

2.3 The Wind Farm Capabilities and Bus Modeling for Static VSA

Consider Fig. 1, which illustrates a schematic of a RSC (rotor-side converter) and a GSC (grid-side converter) coupled to a DFIG. This system can operate temporarily overloaded to contribute to the reactive power support of the system during short-term disturbances.

However, for steady-state operation, DFIG equipped with insulated gate bipolar transistors (IGBTs) that becomes increasingly popular in power control circuits for industrial use, have at synchronous speed operating point a limitation arose due to maximum temperature of the IGBTs junction. This effect causes a reduction in the maximum allowed output current in the RSC (Jung and Hofmann 2011). Consequently, it limits the contribution in reactive power generation that also limits the allowable PF range of the generator. In Brazil, for example, the Brazilian Electricity Regulatory Agency (ANEEL) determines that the PF of wind farms should be in the range of 0.95 inductive and 0.95 capacitive. Thus, this

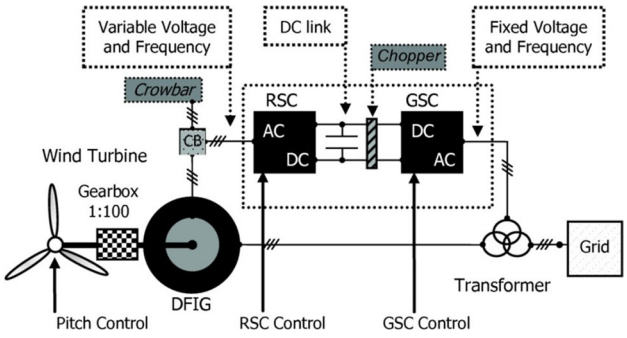

Fig. 1 DFIG with RSC and GSC converters. *Source*: Belati et al. (2013)

PF range determines the contribution limit of each DFIG wind turbine in the reactive power support at the point of interconnection of the system where a wind farm is coupled, aiming at the static voltage stability assessment.

The work presented by Konopinski et al. (2009) proposes the elaboration of the capability curves for a DFIG wind turbines, following a methodology presented in Lund et al. (2007), with a MPPT scheme using the PSF technique and wind turbine parameters detailed in the work. This MPPT technique was applied to a 1.5 MW DFIG wind turbine, and the results obtained through numerical simulations are used to determine the specific speeds (TSR) and the electric power curve generated as a function of the wind speeds. Such MPPT technique is accurately scaled to represent the behavior of a wind farm with DFIG wind turbines (Konopinski et al. 2009).

The DFIG wind farm static capability curves are superimposed for different wind speeds corresponding to variable levels of output power. Figure 2 shows the different capability curves for wind turbine slides s from -0.25 to 0.25, which covers the entire spectrum of wind speeds from the cut-in speed which corresponds to slip s equal to 0.25, until just before the cut-out speed corresponding to the slip s equal to -0.25.

As shown in Fig. 2, the capability curves have a "D" shape; also, manufacturers provide a rectangular capability curve or in a triangular shape delimited by the traced lines of PF = 0.95 (capacitive) and PF = -0.95 (inductive). With respect to the voltage of the wind turbine terminal, which slightly affects the capability curve as discussed in Lund et al. (2007), the voltage limits are established between 0.9 and 1.1 pu as proposed in Martin and Hiskens (2015).

Being necessary to model the DFIG wind farm for its coupling to the PES in order to study the steady-state behavior, the same premise of extending the capability curves of a wind turbine to a wind farm is adopted for bus modeling (Konopinski et al. 2009). The main approaches to modeling DFIG wind farm buses for static VSA purposes are summarized as follows.

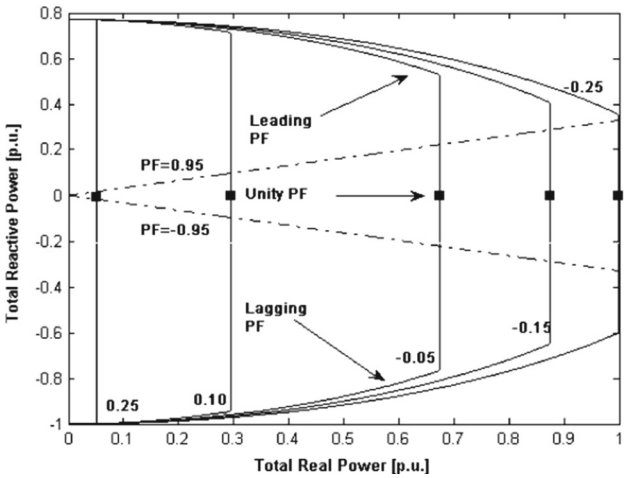

Fig. 2 Wind farm capabilities curves (base: 100 MVA). *Source*: Konopinski et al. (2009)

The PQ bus with negative load representation is one of the most simplified representations of the wind farms. This representation is not indicated for studies of the transient dynamics of the PES. On the other hand, a wind farm bus can also be modeled as a voltage controlled bus (PV) with its operational limits, i.e., its capability curve.

For the purposes of this paper, the representation model used is the PQ bus with negative load. Thus, in this work are presented the results of the simulations with the wind farm model as PQ buses with voltage limits between 0.9 and 1.1 pu, and the power factor between 0.95 inductive and 0.95 capacitive.

3 Static Voltage Stability Assessment (VSA)

In this section, the fundamentals of static VSA are presented, aiming their use in the formulation of the proposed sensitivity index.

An indiscriminate increase in demand can compromise the voltage level in the system buses and, in extreme situation, lead to voltage collapse. Although voltage instability is a dynamic phenomenon, in some cases static analysis tools can be used for its study, which is the case of this work.

Considering that $P_L(\lambda)$ and $Q_L(\lambda)$ are, respectively, the active and reactive power demand vectors in the system buses, parameterized by the load parameter λ, and even considering that $\lambda = 1$ as the current operating point (or the base case demand, λ_0) of the system, the parameterization of the load growth can be written as follows (Colombari et al. 2019).

$$\begin{aligned} P_L(\lambda) &= P_{L_0} + (\lambda - 1) P_{L_0} \\ Q_L(\lambda) &= Q_{L_0} + (\lambda - 1) Q_{L_0}, \end{aligned} \tag{1}$$

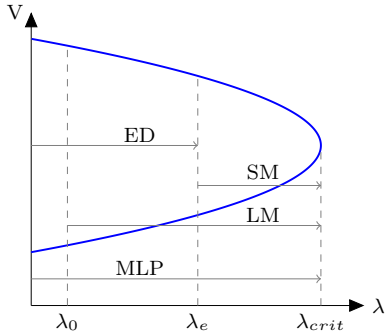

Fig. 3 PV curve and PES operating margins

where P_{L_0} and Q_{L_0} are the active and reactive power demands, respectively, associated with the base case demand of the system. The load flow Eq. (1) with the load growth parameterization can be written in compact form as:

$$F(x, \lambda) = 0, \tag{2}$$

where x is the vector with the power system state variables, i.e., the angles and modules of the voltages, and $F(x)$ is the vector with nonlinear functions of the state variables.

By successively increasing the load parameter λ, and solving the load flow Eq. (2) for each increment of the load parameter, the equilibrium diagram or PV (or λV) curve of the system can be drawn as shown in Fig. 3. The nose point of the PV curve, which is given by $\lambda = \lambda_{\text{crit}}$, represents the maximum load point (MLP) of the system and consists of a bifurcation point. When the system operates closer to the MLP, it is more likely to be subjected to voltage instability. In this context, the voltage stability margin (VSM) or LM is defined as the distance from the current load of the system, λ_0, up to maximum value or the MLP, λ_{crit} (Mansour et al. (2016)).

The continuous power flow (CPF) is considered to be an efficient and accurate method of estimating the MLP and obtaining PV curves, specifically designed to deal with the numerical conditioning problems of the Jacobian matrix of (2) near the MLP. Other margins in the system operation are also known which are identified and positioned in the PV curve in Fig. 3, as the expected demand (ED), λ_e, which is defined as the charge or total demand of the system at a future time close to the current operating point and the security margin (SM) which is the additional load that the system will be able to support starting from the ED until it reaches the MLP.

As previously discussed, the MLP comprises a bifurcation point. There are different types of bifurcations, but the one that is most related to the phenomenon of voltage collapse, which is the focus of the study of this work, is the saddle-node bifurcation (SNB). The sensitivity formulation of this work assumes that the MLP is a SNB. In this type of bifurcation,

the characteristic matrix of load flow equations given by (2) presents a unique null eigenvalue at the SNB point, which allows to mathematically model the occurrence of this type of bifurcation as follows:

$$\begin{aligned} F(x^*, \lambda_{\text{crit}}) &= 0 \\ \nabla F(x^*, \lambda_{\text{crit}})\hat{v} &= 0 \\ \|\hat{v}\| &= 1 \end{aligned} \tag{3}$$

$$\begin{aligned} F(x^*, \lambda_{\text{crit}}) &= 0 \\ \nabla F(x^*, \lambda_{\text{crit}})^{\text{T}}\hat{\omega} &= 0 \\ \|\hat{\omega}\| &= 1, \end{aligned} \tag{4}$$

where $\hat{v}$ and $\hat{\omega}$ are the right and left eigenvectors, respectively, of the characteristic matrix. The SNB is the point x^* in (3) and (4), where the Jacobian singularity of the load flow equations occurs.

After presenting the DFIG wind farm modeling and the phenomenon of voltage stability, the mathematical formulation of the sensitivity is further developed.

4 The Proposed Sensitivity Index of the Loading Margin to the Wind Farm Power Factor

In this section, the formulations of the approximated power factor and the proposed sensitivity index are developed. The sensitivity of the loading margin (LM) in relation to any parameter or control variable of the PES, estimated by linear and quadratic calculations, initially addressed by Greene et al. (1997), proposes that such estimates are used to quickly assess the effectiveness of various control actions to increase the LM. These estimates can provide approximate variations in the LM for changes in each parameter or control variable, requiring the calculation of the SNB bifurcation point for the base case. Although differential equations are the appropriate approach to study the voltage collapse as a consequence of the SNB, it is possible and it is advantageous to calculate the LM and their sensitivities using static equations (Dobson 1994).

Therefore, the formulation used in this paper derives from the SNB bifurcation theory and is based on the approach given by Greene et al. (1997) to estimate the sensitivity of the variation of LM in relation to a specific parameter of interest, which is the power factor of a wind farm coupled to PES.

4.1 Approximate Modified Power Factor

The conventional power factor FP_i for the ith generator bus is given by:

$$\text{FP}_i \triangleq \frac{P_{G_i}}{S_{G_i}} \triangleq \frac{P_{G_i}}{\sqrt{P_{G_i}^2 + Q_{G_i}^2}}, \tag{5}$$

where P_{G_i} and Q_{G_i} are the active and reactive powers generated, respectively, in the ith bus.

A problem with the definition given by (5) is that it does not provide an important data which is the signal of the reactive power. Since it is necessary for the wind farm power factor, to be assessed in the ith bus, to include the reactive power signal in order to determine whether the wind farm is in the capacitive or inductive mode, the power factor including the reactive power signal can be redefined as follows (Cimino and Pagilla 2016).

$$\hat{\text{FP}}_i \triangleq \text{signal}(Q_{G_i})\frac{P_{G_i}}{\sqrt{P_{G_i}^2 + Q_{G_i}^2}}, \tag{6}$$

where

$$\text{signal}(Q_{G_i}) = \begin{cases} 1, & Q_{G_i} \geq 0 \\ -1, & Q_{G_i} < 0 \end{cases}. \tag{7}$$

Even though the redefined power factor (6) allows to determine whether the wind farm is supplying or absorbing reactive power, it has incorporated a discontinuity given by the *signal* function when $Q_{G_i} = 0$, that is, $\lim_{Q\to 0^+} \to \hat{\text{FP}}_i = 1 \neq \lim_{Q\to 0^-} \to \hat{\text{FP}}_i = -1$. To eliminate the discontinuity of $\hat{\text{FP}}_i$, Cimino and Pagilla (2016) still propose the modified power factor, given by the following formulation:

$$\bar{\text{FP}}_i = \text{FP}_i \text{signal}(Q_{G_i}) + [1 - \text{signal}(Q_{G_i})]. \tag{8}$$

The signal function given by (7), and incorporated in (8), can be replaced by an approximate continuous function. Among the various formulations proposed in Tarchala (2011), the one that best fits the contour of the function given by (7) is the sigmoid function $\text{sign}(Q_{G_i}) = \tanh(Q_{G_i}/\varepsilon)$, with the parameter ε set between 0.0012 and 0.015 (depending on the wind farm power for the applications of this work), where $\tanh(\cdot)$ is the hyperbolic tangent function. Therefore, in the sensitivity index modeling, the sigmoid function $\tanh(Q_{G_i}/\varepsilon)$ is adopted as an approximation of the signal function. Thus, the approximated power factor, $\widetilde{\text{FP}}_i$, is formulated as follows.

$$\widetilde{\text{FP}}_i = \text{FP}_i \tanh(Q_{G_i}/\varepsilon) + [1 - \tanh(Q_{G_i}/\varepsilon)], \tag{9}$$

being $\widetilde{\text{FP}}_i$ monotonically decreasing and smooth with respect to the variable Q_{G_i}.

The graph in Fig. 4 highlights the monotony of the approximate modified power factor function, $\widetilde{\text{FP}}_i$, with respect to Q_{G_i}, and shows the slight differences between the curves of the approximated power factor function and the modified power factor function, curves that are practically overlapping

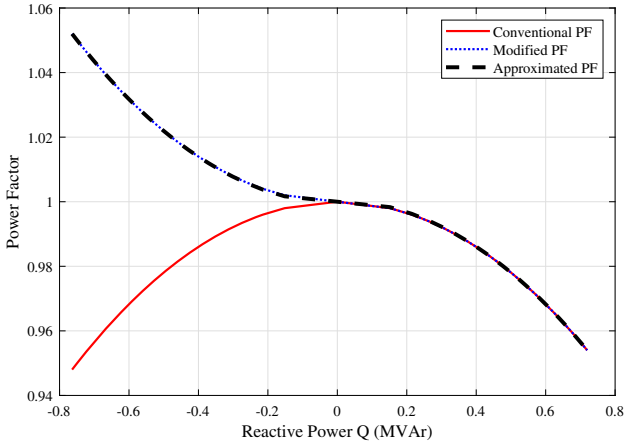

Fig. 4 Modified, approximated and conventional PF

with ε set to 0.0025, which is the appropriate value for the PF range between 0.95 inductive and 0.95 capacitive of the 2.4 MW wind turbine that is used in simulations.

4.2 Formulation of LM Sensitivity to Wind Farm Power Factor

Considering that P_G and Q_G are vectors with the active and reactive powers generated, and P_L and Q_L the vectors with the PES active and reactive demands, respectively, it is possible to write the power balance equations in the form:

$$P_G - P_L = f(x) \tag{10}$$

and

$$Q_G - Q_L = g(x), \tag{11}$$

where the terms $f(x)$ and $g(x)$ are vectors of the active and reactive power flows injected, as a function of the state x. Including the load increment parameter, λ, in terms of the active and reactive loads, it is possible to write:

$$P_L = P_{L_0} + (\lambda - 1)P_{L_0} \tag{12}$$

and

$$Q_L = Q_{L_0} + (\lambda - 1)Q_{L_0}, \tag{13}$$

where P_{L_0} and Q_{L_0} are the active and reactive loads for the base case, respectively. Making the appropriate substitutions from (10) to (13), it is possible to write:

$$P_G - [P_{L_0} + (\lambda - 1)P_{L_0}] - f(x) = 0 \tag{14}$$

and

$$Q_G - [Q_{L_0} + (\lambda - 1)Q_{L_0}] - g(x) = 0. \tag{15}$$

The set of Eqs. (14) and (15) can be written in a compact form as:

$$F(x, \lambda, P_G, Q_G) = 0. \tag{16}$$

Consider that in MLP $X = [x^*, \lambda_{\text{crit}}, P_{G0i}, Q_{G0i}]$, where i indicates the ith bus where the wind farm under test is operating to estimate his sensitivity, and P_{G0i} and Q_{G0i} are the active and reactive generations of this wind farm for the base case. Also consider that only conventional power plants, which do not include any of the wind farms, are participating in the additional redeposing of power. Then, it is possible to obtain a first order approximation of $F(\cdot) = 0$ (from Taylor series expansion) in the form:

$$\left[\frac{\partial F(\cdot)}{\partial x} \quad \frac{\partial F(\cdot)}{\partial \lambda} \quad \frac{\partial F(\cdot)}{\partial P_{G_i}} \quad \frac{\partial F(\cdot)}{\partial Q_{G_i}}\right]\Big|_X \begin{bmatrix} \Delta x \\ \Delta\lambda \\ \Delta P_{G_i} \\ \Delta Q_{G_i} \end{bmatrix} = 0. \tag{17}$$

The solution of the system of (17), which is obtained in the MLP, results in a singular Jacobian matrix, $J_x\big|_X$; that is, it has a unique null eigenvalue, and considering ω as being the eigenvector associated with the null eigenvalue, then $\omega^{\mathrm{T}} J_x\big|_X = 0$. So, the following formulation may be structured:

$$\omega^{\mathrm{T}} T_1^{-1} T_2\Big|_X \Delta\lambda + \omega^{\mathrm{T}} T_1^{-1} T_3\Big|_X \Delta P_{G_i} + \omega^{\mathrm{T}} T_1^{-1} T_4\Big|_X \Delta Q_{G_i} = 0, \tag{18}$$

where $T_1 = \frac{\partial F(\cdot)}{\partial x}(J_x\big|_X)^{-1}$, $T_2 = \frac{\partial F(\cdot)}{\partial \lambda}$, $T_3 = \frac{\partial F(\cdot)}{\partial P_{G_i}}$ and $T_4 = \frac{\partial F(\cdot)}{\partial Q_{G_i}}$.

Equation (18) provides a relation between the differential loading $\Delta\lambda$ of the PES and the differences in the active power generation ΔP_{G_i} and the reactive power generation ΔQ_{G_i}, on the ith bus, for the MLP.

This relation can be used to analyze the sensitivity between the loading variation and the power factor of wind farm in the ith bus, which is a function of ΔP_{G_i} and ΔQ_{G_i}. One approach is to consider the sensitivity analysis between $\Delta\lambda$ and ΔP_{G_i} holding $\Delta Q_{G_i} = 0$, and the other is between $\Delta\lambda$ and ΔQ_{G_i} while holding $\Delta P_{G_i} = 0$. These approaches applied to (18) result in:

$$\Delta P_{G_i} = -\frac{\omega^{\mathrm{T}} T_1^{-1} T_2}{\omega^{\mathrm{T}} T_1^{-1} T_3}\Big|_X \Delta\lambda, \tag{19}$$

where $\Delta\lambda = \lambda_{\text{crit}} - \lambda$, e $\Delta P_{G_i} = P_{G_i} - P_{G_{0i}}$, and

$$\Delta Q_{G_i} = -\left.\frac{\omega^{\mathrm{T}} T_1^{-1} T_2}{\omega^{\mathrm{T}} T_1^{-1} T_4}\right|_X \Delta\lambda, \tag{20}$$

where $\Delta Q_{G_i} = Q_{G_i} - Q_{G_{0i}}$.

On the other hand, by regrouping the terms of the approximated power factor, $\widetilde{\text{FP}}_i$, the function s_i can be defined as follows:

$$\begin{aligned} & s_i(\widetilde{\text{FP}}_i, P_{G_i}, Q_{G_i}) \\ & = \widetilde{\text{FP}}_i - \frac{P_{G_i}}{\sqrt{P_{G_i}^2 + Q_{G_i}^2}} \tanh(Q_{G_i}/\varepsilon) \\ & \quad -[1 - \tanh(Q_{G_i}/\varepsilon)] = 0. \end{aligned} \tag{21}$$

Equation (21) must also be linearized in Taylor series in the MLP. That results in:

$$\begin{aligned} \Delta\widetilde{\text{FP}}_i = & -\left.\frac{\partial s_i(\widetilde{\text{FP}}_i, P_{G_i}, Q_{G_i})}{\partial P_{G_i}}\right|_X \Delta P_{G_i} \\ & -\left.\frac{\partial s_i(\widetilde{\text{FP}}_i, P_{G_i}, Q_{G_i})}{\partial Q_{G_i}}\right|_X \Delta Q_{G_i}. \end{aligned} \tag{22}$$

Making the appropriate substitutions from (18) to (22), it can get the following expression.

$$\begin{aligned} S_i = \frac{\Delta\lambda}{\Delta\widetilde{\text{FP}}_i} = & \left[\left(\frac{\partial s_i(\widetilde{\text{FP}}_i, P_{G_i}, Q_{G_i})}{\partial P_{G_i}} \frac{\omega^{\mathrm{T}} T_1^{-1} T_2}{\omega^{\mathrm{T}} T_1^{-1} T_3}\right)\right|_X \\ & + \left.\left(\frac{\partial s_i(\widetilde{\text{FP}}_i, P_{G_i}, Q_{G_i})}{\partial Q_{G_i}} \frac{\omega^{\mathrm{T}} T_1^{-1} T_2}{\omega^{\mathrm{T}} T_1^{-1} T_4}\right)\right|_X\Bigg]^{-1}. \end{aligned} \tag{23}$$

Formulation (23) is the one used to estimate the sensitivity of the variation of the LM in relation to the power factor of the wind farm connected to the ith bus. The computational implementation for the calculation of the sensitivity S_i is obtained by the previous calculation of Jacobian of the power flow equation system for the SNB point and, subsequently, by calculations of the eigenvector ω, the matrix T_1 and the vectors T_2, T_3 and T_4.

All the computational routines needed to provide the numerical results shown in this paper were implemented using MATLAB software. Also, the computation of the maximum load point, which is necessary to calculate the sensitivity index, was done by means of the PSAT MATLAB Toolbox (Milano 2006).

5 Simulation Results

In this section, the results of the simulations are detailed with the application of the proposed sensitivity index for a 56-bus system that corresponds to a part of the NE subsystem of the SIN, which is powered predominantly by wind generation.

5.1 Description of the 56-Bus Test System

The SIN has, currently, a total wind power generation capacity of 14.8 GW distributed in 580 wind farms, which comprises a total of 7500 wind turbines. From this, total of wind power generation capacity 12.05 GW is located in the NE subsystem, with the maximum recorded generation of 8.87 GW (on an hourly basis) on November 18, 2018, with capacity factor of 83.39% and load factor of 100.71%; that is, on that day the NE subsystem exported wind power generation to the SIN (Operador Nacional do Sistema Elétrico ONS 2019).

Based on this high penetration of wind farms in operation and with a forecast of coupling of others wind farms in the short (1 year) and medium term (5 years), a part of the NE subsystem was chosen to elaborate the proposed 56-bus test system. The chosen area includes parts of the states of Rio Grande (RN) and Paraiba (PB), which contain 22 wind farms with 234 wind turbines, including those already exist and those that will be coupled in the short term, as shown in the line diagram in Fig. 5. This line diagram includes each of the wind farm capacities in MW, the demands on the 9 load buses, and the original buses and wind farm names in the NE subsystem to facilitate their locations in the SIN's Geographical Information System dynamic map (Operador Nacional do Sistema Elétrico ONS 2019).

The formulated test system with 56 buses of this part of the NE subsystem includes a total demand of 594.04 MW, assuming a non-wind generation of 296.19 MW from the 51-JESOPER-RN013 thermal plant, which is adopted as reference bus. Also it is assumed a total wind generation of 312.73 MW corresponding to 50% of the installed capacity of the 22 wind farms, aiming at the additional redeposing of power of those wind farms indicated by the sensitivity ranking, proposed as a voltage preventive control. It can be observed that if wind generation is raised to 100%, it could generate 521.57 MW, that is, close to serving 100% of the total load of 594.04 MW, as occurred in the NE subsystem on November 18, 2018. Some important data and information of this test system, in the base case of operation, are:

- Total demand: 594.04 MW distributed in 9 buses
- Number of thermal generator: 1 with 289.57 MW
- Number of wind farms: 22
- Number of wind turbines: 234
- Wind power generation: 319.37 MW
- The power factor of each wind farm (wind farm PF) was initially set to 1.0
- Rate wind generation/total generation: 52.45%
- Loading Margin from the base case: 88.86 MW.

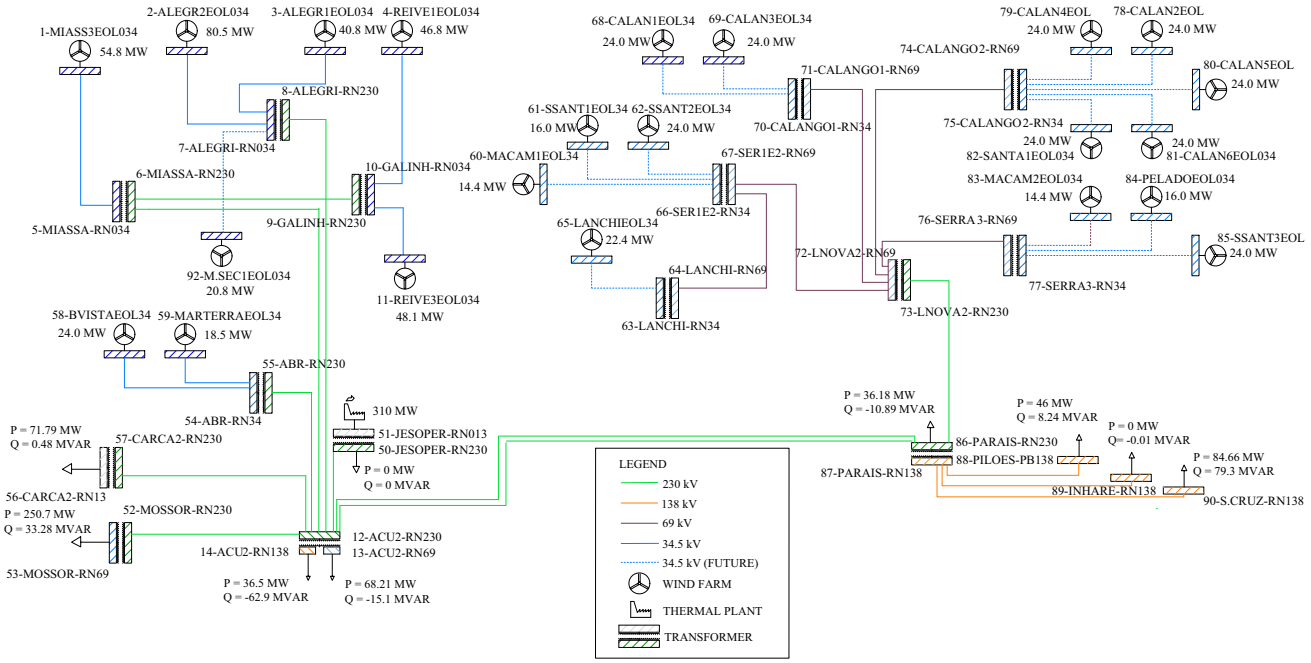

Fig. 5 Line diagram of 56-bus test system

Each wind farm is represented by an equivalent wind turbine with power equal to the sum of the individual powers of all wind turbines in the farm. The system loads are coupled on 9 buses where the active and reactive powers are delivered to the rest of the NE subsystem, for example to the buses 14-ACU-RN138 and 53-MOSSOR-RN069, shown in Fig. 5.

For this test system, the proposed sensitivity index was calculated for each wind farm, in order to rank the units that most significantly impact the system's LM through its power factor control. The results are presented in the next subsection.

5.2 Results and Voltage Preventive Control Actions

The load flow and the CPF for the base case of the 56-bus system test were performed with the power factor set at 1.0 for all wind farms, in order to determine the base case LM which serves as a comparative reference for the increases in LM that is obtained with the adjustment in the power factors of the wind farms.

Since the range of the wind farm PFs is from 0.95 inductive to 0.95 capacitive, in this paper the sensitivity calculations made for each of the wind farms with each of the following four PF adjustments: 0.99 and 0.95 inductive, and 0.95 and 0.99 capacitive. This is to determine in which PF a given wind farm has its highest sensitivity. For example, Table 1 shows the calculated sensitivities of the wind farm 58-BVISTAEOL34. Negative and positive values of PF indicate an inductive and capacitive power generation by wind farm, respectively.

Table 1 58-BVISTAEOL34 wind farm sensitivities

Wind farm name	Wind farm PF	Sens. S_i
58-BVISTAEOL34	− 0.99	0.1047
58-BVISTAEOL34	− 0.95	0.0339
58-BVISTAEOL34	0.95	0.4173
58-BVISTAEOL34	0.99	0.3275

Table 2 Ranking of wind farms by sensitivities

Wind farm name	Wind farm PF	Sens. S_i
58-BVISTAEOL34	0.95	0.4173
59-MARTERRAEOL34	0.95	0.2915
1-MIASS3EOL034	0.99	0.1060
11-REIVE3ELO034	0.99	0.0933
4-REIVE1ELO034	0.99	0.0886
2-ALEGR2EOL034	0.99	0.0577

The sensitivity calculations by the proposed method results in the ranking shown in Table 2, which indicates the order of the first six wind farms that can best contribute to the increase the LM. The PF in Table 2 corresponds to the wind farm PF which resulted in the highest sensitivity for that wind farm.

Figure 6 shows the voltage profiles of the 20 buses electrically closest to the critical bus 53-MOSSOR-RN069. Two voltage profiles are presented, one for the base case and the other with the wind farm 58-BVISTAEOL34 PF setting in

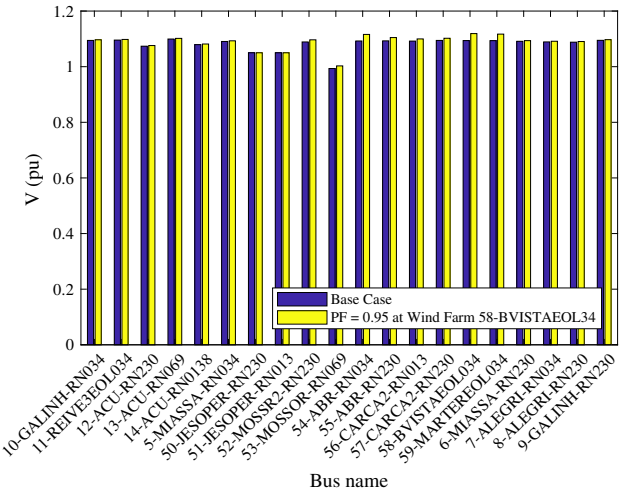

Fig. 6 Voltage profiles for power flows in the base case and with PF = 0.95 in the most sensitive wind farm

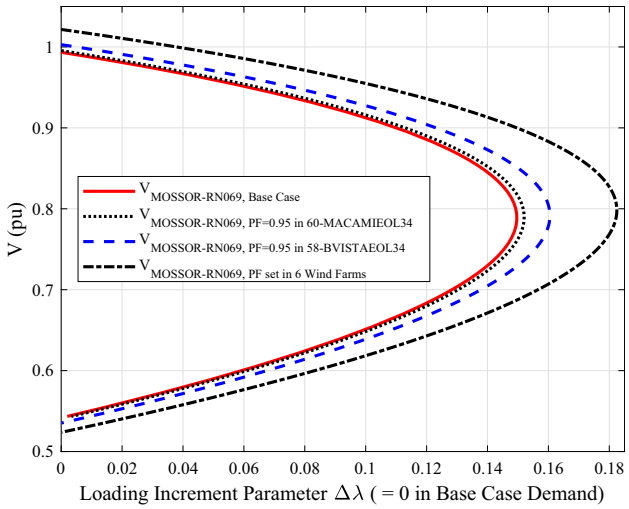

Fig. 7 Critical bus 53-MOSSOR-RN069 PV curves

Table 3 LM increments by wind farm sensitivities

Wind farm name	Increments in LM	Sens. S_i
58-BVISTAEOL34	0.0132	0.4173
59-MARTERRAEOL34	0.0118	0.2915
1-MIASS3EOL034	0.0097	0.1060
11-REIVE3ELO034	0.0095	0.0933

0.95 capacitive, the most sensitive according to Table 2. It can be observed a slight increase in the critical bus voltage module with the wind farm 58-BVISTAEOL34 PF setting in 0.95 capacitive.

Table 3 shows the increment in the LM, from base case, by adjusting the PF of each wind farm, separately, in its higher-sensitivity PF adjustment, to highlight a pattern that the larger increase in LM occurs when adjusting the PFs of the most sensitive wind farms. Ultimately, Fig. 7 shows the PV curves of the critical bus for CPFs applied first to the base case, while the second is with the less sensitive wind farm 60-MACAMIEOL34 PF setting in 0.95 capacitive, the third is with 58-BVISTAEOL34 the most sensitive wind farm with PF in 0.95 capacitive, and the fourth is with the most 6 sensitives wind farms having their power factors adjusted according to Table 2.

Therefore, through the rankings of the sensitivity index as shown in Table 2, it can be determined which wind farms should have their PF adjusted as voltage preventive control actions in order to contribute to the increase in the loading margin and, consequently, to improve the static voltage stability.

6 Conclusions

In this paper, a voltage preventive control actions based on the ranking of wind farms that most significantly impact the system's LM through the control of its power factor were proposed. A sensitivity index, whose developed mathematical formulation was based on a linear approximation of the power balance equations in the vicinity of the MLP, was used to rank those wind farms.

To test this proposal, a 56-bus test system based on real data from the NE subsystem of the SIN was used, which comprises 22 wind farms. The results obtained in the simulations indicate the feasibility of applying this proposal to calculating the LM sensitivities to the wind farm power factors.

Also, by analyzing the results, it has been shown that it is possible to use this ranking of the sensitivity index, when indicating the most sensitive wind farms that must be adjusted their power factors as voltage preventive control actions aiming to contribute in the increment of the LM.

The next activities of this research aim at the development of a voltage preventive control strategy based on the maximization of the system's LM by means of optimal power flow techniques. Also, the results obtained from the proposed static voltage preventive control can be used by dynamic stability assessment algorithms, in order to assess in what way the changes in the operating point of these wind farms affect the dynamic response of the system in terms of dynamic stability indexes.

References

Abdelrahem, M., & Kennel, R. (2016). Fault-ride through strategy for permanent-magnet synchronous generators in variable-speed wind turbines. *Energies*, *9*(12), 1066.

Baghsorkhi, S. S. (2015). Computing saddle-node and limit-induced bifurcation manifolds for subtransmission and transmission wind generation. In *Power and Energy Society General Meeting*, 2015 IEEE (pp. 1–5). IEEE

Belati, E. A., Sguarezi Filho A. J., Salles, M. B. C., Adélia, R. S., & Gualberto, L. (2013). Analysis of reactive power capability for doubly-fed induction generator of wind energy systems using an optimal reactive power flow.

Cimino, M., & Pagilla, P. R. (2016). Reactive power control for multiple synchronous generators connected in parallel. *IEEE Transactions on Power Systems*, *31*(6), 4371–4378.

Colombari, L., Kuiava, R., Peric, V., & Ramos, R. A. (2019). Continuation load flow considering discontinuous behaviors of distribution grids. *IEEE Transactions on Power Systems*, *1*, 1.

Dobson, I. (1994). The irrelevance of load dynamics for the loading margin to voltage collapse and its sensitivities. In *Sensitivities* (vol. 29, pp. 509–518).

Gao, B., Morison, G. K., & Kundur, P. (1992). Voltage stability evaluation using modal analysis. *IEEE Transactions on Power Systems*, *7*(4), 1529–1542.

Greene, S., Dobson, I., & Alvarado, F. L. (1997). Sensitivity of the loading margin to voltage collapse with respect to arbitrary parameters. *IEEE Transactions on Power Systems*, *12*(1), 262–272.

Hatziargyriou, N., Van Cutsem, T., Milanović, J., Pourbeik, P., Vournas, C., Vlachokyriakou, O., Kotsampopoulos, P., Ramos, R., Boemer, J., Aristidou, P., et al. (2017). Contribution to bulk system control and stability by distributed energy resources connected at distribution network. *IEEE*.

Hu, J., Li, Y., & Zhu, J. (2019). Multi-objective model predictive control of doubly-fed induction generators for wind energy conversion. *IET Generation, Transmission Distribution*, *13*(1), 21–29.

Jung, J., & Hofmann W. (2011). Investigation of thermal stress in the rotor of doubly-fed induction generators at synchronous operating point. In *2011 IEEE international electric machines drives conference (IEMDC)* (pp. 896–901).

Konopinski, R. J., Vijayan, P., & Ajjarapu, V. (2009). Extended reactive capability of DFIG wind parks for enhanced system performance. *IEEE Transactions on Power Systems*, *24*(3), 1346–1355.

Lalouni, S., Rekioua, D., Idjdarene, K., & Tounzi, A. M. (2014). An improved MPPT algorithm for wind energy conversion system. *Journal of Electrical Systems*, *10*(4), 484.

Lund, T., Sørensen, P., & Eek, J. (2007). Reactive power capability of a wind turbine with doubly fed induction generator. *Wind Energy: An International Journal for Progress and Applications in Wind Power Conversion Technology*, *10*(4), 379–394.

Mansour, M. R., Alberto, L. F. C., & Ramos, R. A. (2016). Preventive control design for voltage stability considering multiple critical contingencies. *IEEE Transactions on Power Systems*, *31*(2), 1517–1525.

Martin, J. A., & Hiskens, I. A. (2015). Reactive power limitation due to wind-farm collector networks. In *2015 IEEE Eindhoven PowerTech* (pp. 1–6).

Meegahapola, L., Littler, T., & Perera, S. (2013). Capability curve based enhanced reactive power control strategy for stability enhancement and network voltage management. *International Journal of Electrical Power and Energy Systems*, *52*, 96–106.

Meegahapola, L. G., Littler, T., & Flynn, D. (2010). Decoupled-DFIG fault ride-through strategy for enhanced stability performance during grid faults. *IEEE Transactions on Sustainable Energy*, *1*(3), 152–162.

Milano, F. (2006). An open source power system analysis toolbox. In *Power engineering society general meeting*, 2006. IEEE (p 1). IEEE.

Operador Nacional do Sistema Elétrico ONS. (2019). Boletim mensal de geração eólica - dezembro/2018, p. 9.

Operador Nacional do Sistema Elétrico ONS. (2019). Mapa dinámico - sistema de informações geográficas cadastrais. http://www.ons.org.br/paginas/sobre-o-sin/mapas/.

Raza, K. S. M., Goto, H., Guo, H.-J., & Ichinokura O. (2008). A novel algorithm for fast and efficient maximum power point tracking of wind energy conversion systems. In *2008 18th international conference on electrical machines* (pp. 1–6).

Seydel, R. (2009). *Practical bifurcation and stability analysis* (Vol. 5). Berlin: Springer.

Simoes, M. G., Bose, B. K., & Spiegel, R. J. (1997). Fuzzy logic based intelligent control of a variable speed cage machine wind generation system. *IEEE Transactions on Power Electronics*, *12*(1), 87–95.

Sl-Subhi, A., Alsumiri, M., & Alalwani S. (2017). Novel MPPT algorithm for low cost wind energy conversion systems. In *2017 international conference on advanced control circuits systems (ACCS) systems, 2017 international conference on new paradigms in electronics information technology (PEIT)* (pp. 144–148).

Tamimi, B., Cañizares, C., & Bhattacharya, K. (2011). Modeling and performance analysis of large solar photo-voltaic generation on voltage stability and inter-area oscillations. In *Power and energy society general meeting*, 2011 IEEE, pp. 1–6. IEEE

Tarchala, G. (2011). Influence of the sign function approximation form on performance of the sliding-mode speed observer for induction motor drive. In *2011 IEEE international symposium on industrial electronics (ISIE)*, pp 1397–1402. IEEE

Van Cutsem, T. (2000). Voltage instability: Phenomena, countermeasures, and analysis methods. *Proceedings of the IEEE*, *88*(2), 208–227.